2021 43rd Annual International Conference of the
IEEE Engineering in Medicine & Biology Society (EMBC)
Oct 31 - Nov 4, 2021. Virtual Conference

Heart Rate and Respiratory Rate Monitoring Using Seismocardiography

Po-Ya Hsu,[1] Po-Han Hsu,[1] Tsung-Han Lee[1] & Hsin-Li Liu[2*]

Abstract— **Vital signs monitoring is critical for healthcare. Currently, at-home vital signs monitoring is obstructed by the complicated device, unaffordable cost, and inconvenience. In this study, we develop a simultaneous heart rate and respiratory rate monitoring technique that requires only one tri-axial accelerometer placing on the sternum. We devise a signal processing technique to generate seismocardiography and respiratory vibration from the raw acceleration data; furthermore, we formulate the algorithms to compute the heart rate and respiratory rate from the processed signals. We tested the methodology on 20 young healthy adults during pre-exercise and post-exercise sitting. The accuracy of** 98.3% **and** 97.3% **are achieved in heart rate monitoring during pre-exercise and post-exercise sitting. For respiratory rate, an accuracy of** 96.8% **is accomplished. Given the accuracy, affordable cost and convenience, the acceleration-based technique shows great promise for at-home vital signs monitoring.**

Clinical relevance— **Portable heart rate and respiratory rate monitoring is substantial in elevating the quality of healthcare environment.**

I. INTRODUCTION

Vital sign monitoring is essential for health evaluation and enhance early detection of cardiovascular disease. Accessible accurate heart rate monitoring has the potential to decrease the global mortality rate and reduce the economic loss [1]. In addition to heart rates, real-time respiratory rate monitoring is substantial for the preventive care of the COVID-19.

Numerous techniques have been proposed to monitor heart rates, including electrocardiography (ECG), photoplethysmography (PPG), ballistocardiography (BCG), and seismocardiography (SCG). ECG has been known to be challenging for an untrained user to implement in a domestic environment. Plus, ECG is not suitable for long-term usage due to the irritation caused by the electrodes. PPG is relatively easy to use, but intra-beat information is difficult to be extracted from PPG [2]. Additionally, PPG is easily corrupted by motion artifacts [3]. While BCG captures the morphology of the mechanical cardiac activity, it cannot be measured by a portable device [4]. SCG records the dorsal-ventral motion induced by the heart's contraction and ejection of the blood from the ventricles to the vascular tree. More importantly, SCG can be detected by placing an accelerometer on the chest. Nevertheless, removing the motion artifacts from SCG still remains as a challenging task.

This work was not supported by any organization.

[1]Po-Ya Hsu, Po-Han Hsu and Tsung-Han Lee are with the Department of Computer Science & Engineering, University of California, San Diego, The USA

[2]Hsin-Li Liu is with the Department of Nursing, Central Taiwan University of Science and Technology, Taiwan

[*]Hsin-Li Liu is the corresponding author hlliu@ctust.edu.tw

Few studies report promising results using SCG to monitor heart rates [2], [5], [6]. In Wahlstrom et al.'s study [5], hidden Markov models (HMM) are applied. While in Tadi et al.'s research, Hilbert transform is performed on the SCG signal for heart rate estimation. State-of-the-art achievement has been made by DMellos et al. with leveraging both SCG and gyrocardiography (GCG). Although successful heart rate monitoring is achieved, all require the humans lying on the bed during measurement.

In this study, we demonstrate adopting SCG data for both heart rate and respiratory rate monitoring. Our strategy allows the person to sit normally in a chair during monitoring. We show the efficacy of the proposed methodology in 20 young healthy adults.

II. METHODS

We start with the description of our data collection method. Subsequently, we dive into the sensor data processing step. Following that, we present our heartbeat labeling and respiratory rate computation algorithm. Finally, we elaborate on how we quantify the performance of the proposed methodology.

A. Data Collection

This study was approved by the Jen-Ai Hospital-Joint Institutional Review Board. We recruited 20 young healthy volunteer to undergo the data acquisition process. All 20 subjects provided the written informed consent to participate in the study on their own will. The age of the recruited participants lies within $25-32$ years, and the gender distribution is 6 females and 14 males.

TABLE I
DESIGN OF EXPERIMENTS

Activities	sitting before & after a 3-minute exercise
Duration	each activity lasts for 3 minutes
Sensor Placement	at the bottom of the sternum
Description	participants wear the sensor throughout the whole experiment
Sensor	one tri-axial accelerometer
Measurements	accelerations, heart and respiratory rates

We summarize the experimental design in Table I. All the participants went through two activities: sitting before and right after a 3-minute walking exercise. For each activity, the participant stays as still as possible in the same posture for three minutes with the wearable sensor placed on the body. As for the walking exercise, the participants are asked

to walk consistently and continuously at their normal pace for three minutes.

The collected data include body acceleration, heart rate, and videoed respiratory rate. Throughout the whole experiment, the acceleration data are measured with the sensor placed on the participant's sternum (as shown in Fig. 1). The acceleration sensor is MPU-6050 [7], and the data sampling rate is 150Hz. During the two sitting activities, the heart rate is measured using Rossmax MG150f. This blood pressure monitor was certified by European Society of Hypertension and clinically validated by British Hypertension Society with an A/A grade. All the data acquisition was completed by the same person, who was well trained by an experienced registered nurse to perform the measuring. Moreover, before the start of each activity, the same person inspected all the sensor to be well-functioning. The referenced respiratory rate was collected through video-recording the subject's normal breathing while sitting still in the chair.

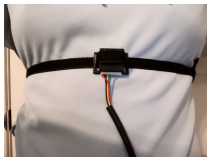

Fig. 1. Accelerometer placed on the sternum.

B. Sensor Data Processing

We process and decompose the raw acceleration signals into two datasets - one set for heart rate and the other for respiratory rate computation. For heart rate, we develop a three-step signal processing procedure. First, for vertical and dorsal-ventral acceleration, we remove the low-frequency motion artifact with a third-order Savitzky-Golay filter of 100ms span, which has been shown effective in removing running motion artifact in [8]. Next, we clean the high-frequency noise with a sixth-order low-pass Butterworth filter. We set the cut-off frequency at 35Hz, which is often used in ballistocardiogram and SCG extraction [7]. Finally, we smooth the data through interpolation with spline cubic curves at 750Hz. We demonstrate the raw and processed acceleration signals in Fig. 2.

For breathing rate data generation, our proposed strategy is similar to the heart rate data processing. Different from heart rate dataset, we utilize only the dorsal-ventral acceleration signal for respiratory rate computation. In the first step, we take the residual of the Savitzky-Golay filtered heart rate data, which is a byproduct in the first step of the heart rate dataset construction. Subsequently, we remove the data offset, which is caused by the gravity and other constant motion effect. Next, we pass the processed data into a sixth-order low-pass Butterworth filter with a 0.5 Hz cutoff frequency. Eventually, we perform interpolation at 750Hz to smooth the data.

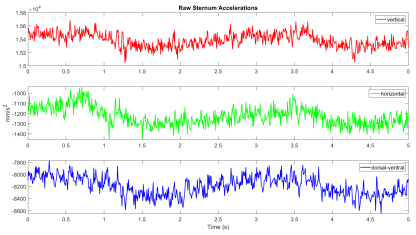

(a) Raw Data

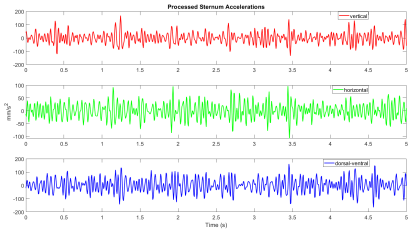

(b) Processed Data

Fig. 2. Demonstration of raw and processed acceleration data. Red: Vertical; Green: Horizontal; Blue: Dorsal-ventral

C. Heart Rate Computation

There are mainly five steps in our heart rate computation algorithm: 1) initial heartbeat labeling, 2) waveform-based heartbeat detection, 3) false positive heartbeat removal, 4) search-back for the missing heartbeat, and 5) heart rate estimation.

Initial heartbeat labeling: We first input the vertical and dorsal-ventral accelerations into our Heartbeat Labeling Algorithm (1) separately, and then we sift the peaks that deviate less than 10ms between vertical and dorsal-ventral accelerations as the valid heartbeats. The concept behind the algorithm is to identify the maximum peak in each empirically reasonable time window, which is also used in other heartbeat detection studies [8], [7].

Waveform-based heartbeat detection: In this step, we utilize the waveform to correct the potential erroneous or miss-labeled heartbeats from Step 1, which is an approach shown to be effective in [9]. Based on the fact that noise-removed SCG is a quasi-periodic signal, we derive the envelope of the dorsal-ventral acceleration to capture the signal's intrinsic quasi-periodicity. Such envelope is determined using spline interpolation over local maxima separated by at least samples of 200ms. If there exists no heartbeat peak in an envelope, we mark the maximum peak as heartbeats. In another case, if there are multiple heartbeats detected in an envelope, we remove heartbeats inside this envelope.

False positive heartbeat removal: In this process, we remove the false positive heartbeats. We compute the heartbeats' intervals and consider only the interval lying within $0.5s - 1.2s$ as reasonable period. Subsequently, we calculate the mean and standard deviation (STD) of the selected intervals. Last, we remove the false positive heartbeats, which are those with intervals being less than $mean - STD$.

Search-back for the missing heartbeat: Some heartbeat peaks could have been falsely removed in the previous pro-

Algorithm 1: Heartbeat Labeling Algorithm

```
Input: One-dimensional Acceleration Data D
Output: Heartbeat Peaks indices
Initialize the size of the sliding window;
peaks = [ ];
current = 1s;
delay = 0.5s;
window = sampling_rate;
while current + window < D.size do
    if peaks.is_empty then
        start = 1;
        last = window;
    else
        start = current + delay;
        last = current + window;
    end
    current = start + D[start:last].max_index;
    peaks.push(current-1);
end
```

cess, and in this procedure, we search the missing heartbeats back. We identify the heartbeats as missing when we detect an interval of two consecutive heartbeats being longer than 1.2s. Next, we compute the number of heartbeats to be detected through peak-to-peak length estimation as we did in the previous step. Eventually, we enforce the number of heartbeats and label the missing heartbeats within the selected interval using Algorithm 1.

Heart rate estimation: We average out the interval length between every two consecutive heartbeats and round the number to obtain the heart rate of a subject.

D. Respiratory Rate Computation

We apply Fourier Transform and spectrum peak detection to conduct respiratory rate estimation. Once we acquire the respiration-oriented processed dorsal-ventral acceleration, we use Fourier Transform directly on the processed signal. Following that, we search the peak near 0.2 - 0.4 Hz on the frequency spectrum. Eventually, we treat the frequency that produces the largest peak near the specified range as the respiratory rate.

E. Performance Evaluation

We compare the estimations with the ground truth to evaluate the performance of the proposed algorithms. For heart rate, we calculate the accuracy by using the expression $\frac{estimation}{real\,heart\,rate} \times 100\%$. For respiratory rate, we first compute the true respiratory rate through the video-recording, and then adopt the accuracy metric to evaluate the algorithm. Moreover, we will visualize the different respiratory rates of the same subject in two different activities: sitting still pre-exercise versus post-exercise.

III. Results & Discussion

We first exhibit the heart rate and respiratory rate accuracy of the 20 participants in Table II. Following that, we present the visualization of the combined signals and respiratory rate in different activities. Finally, we compare the averaged accuracy with other existing SCG-based methods in Table III.

TABLE II
RESULTS OF THE HEART RATE AND RESPIRATORY RATE ESTIMATION MODELS

Subject	Accuracy of sitting heart rate (%)	Accuracy of post-exercise heart rate (%)	Accuracy of sitting respiratory rate (%)
1	98.9	98.9	≈ 100
2	100	78.7	≈ 100
3	98.6	98.7	≈ 100
4	95.7	90.3	≈ 100
5	96.6	99.0	≈ 85
6	100	98.6	≈ 100
7	100	100	≈ 100
8	100	96.8	≈ 100
9	100	98.7	≈ 100
10	100	98.7	≈ 80
11	100	100	≈ 100
12	91.7	100	≈ 100
13	98.6	100	≈ 85
14	93.0	93.1	≈ 100
15	100	98.7	≈ 100
16	98.8	96.7	≈ 85
17	98.5	100	≈ 100
18	98.7	100	≈ 100
19	100	98.8	≈ 100
20	96.5	100	≈ 100
overall	98.3	97.3	≈ 96.8

A. Efficacy of Heart Rate Estimation

According to the accuracy numbers in Table II, we observe higher heart rate accuracy in sitting still compared to sitting after walking. In sitting still activity, every estimated heart rate reaches an accuracy greater than 90%, and overall, the model accomplishes an accuracy of 98.3%. Conversely, sitting post-exercise generates larger error in average. One subject appears to have a badly estimated heart rate ($< 80\%$). Nevertheless, the heart rate estimation model still achieves an accuracy of 97.3% in post-exercise heart rate estimation. In addition, we display an example of labeled heartbeats in Fig. 3. From the figure, we can perceive the quasi-periodic heartbeat peaks labeled in the SCG with the devised algorithm.

B. Efficacy of Respiratory Rate Estimation

We present the accuracy of respiratory rate in Table II, exhibit combined heartbeats and breathing acceleration in Fig. 3, and display the respiratory rates of two activities in Fig. 4. Promising results are observed from both the table and the figures. From the table, we are able to showcase that the model has successfully estimated sixteen out of twenty participants with nearly 100% accuracy. When comparing post-exercise respiratory rate to sitting still, we observe sharp increase in 95% of the participants in Fig. 4. Subject 4's respiratory rate does not surge in post-exercise activity, and it might be due to the fact that Subject 4 jogs on a regular daily basis.

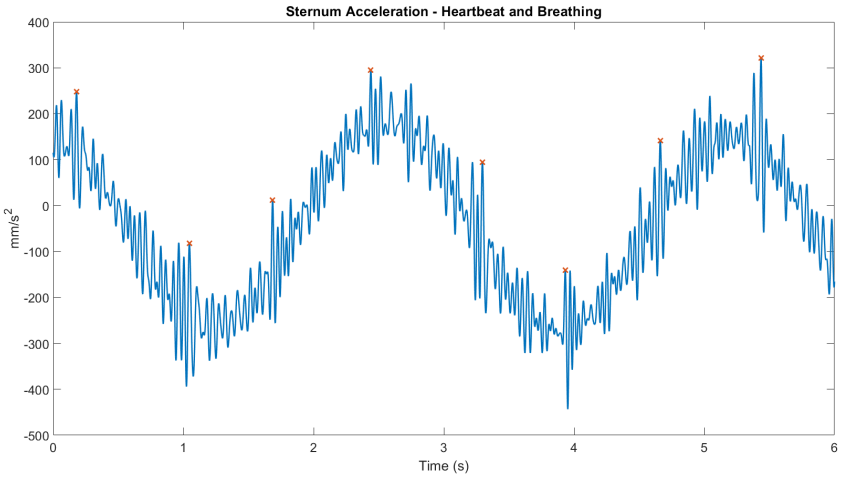

Fig. 3. Visualization of both labeled heartbeats and breathing data. Red asterisks are the heartbeat peaks labeled by our algorithm.

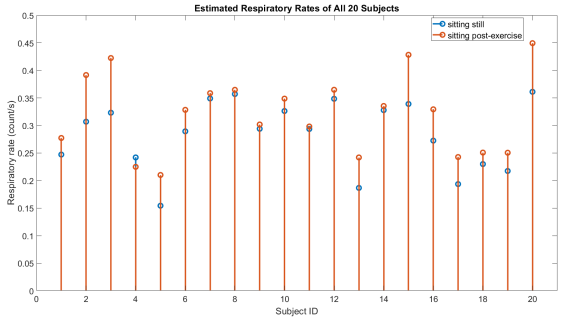

Fig. 4. Visualization of respiratory rate in before versus after exercise. Blue circle stands for pre-exercise, and red circle for post-exercise.

C. Comparison with State-of-the-Art Works

TABLE III
COMPARISON OF HEART RATE ACCURACY TO STATE OF THE ART

Method	Accuracy	Posture
Hidden Markov Model SCG [5]	98.5	Supine
Hilbert Transform SCG [6]	99.4	Supine
SCG + GCG [2]	99.8	Supine
Ours - multi-channel SCG	98.3	**Sitting still**
Ours- multi-channel SCG	97.3	**Sitting post-exercise**

We demonstrate the competitiveness of the proposed heart rate estimation model by comparing the results with the state-of-the-art works that also utilize SCG to compute heart rates. The highest accuracy is achieved by D'Mello et al. using SCG and gycocardiography together to estimate the heart rate [2]. However, all the existing studies require the participants to stay in a supine position. Such posture restricts the subjects from performing normal activity. In our proposed methodology, we successfully achieve $> 97\%$ accuracy in the sitting posture. More importantly, it does not matter whether the person is sitting still or panting in the chair due to the exercise.

IV. CONCLUSIONS

We devise a seismocardiogram-based methodology that can accurately monitor the heart rate and respiratory rate. We demonstrate that such method is both ultra-convenient and cost-efficient in 20 young healthy participants, which requires only one sensor placing on the sternum. More importantly, the person can sit normally in a chair during monitoring. Based on the results, wearable SCG may be promising to apply in both daily and clinical monitoring.

REFERENCES

[1] D. E. Bloom, E. Cafiero, E. Jané-Llopis, S. Abrahams-Gessel, L. R. Bloom, S. Fathima, A. B. Feigl, T. Gaziano, A. Hamandi, M. Mowafi, *et al.*, "The global economic burden of noncommunicable diseases," Program on the Global Demography of Aging, Tech. Rep., 2012.

[2] Y. D'Mello, J. Skoric, S. Xu, P. J. Roche, M. Lortie, S. Gagnon, and D. V. Plant, "Real-time cardiac beat detection and heart rate monitoring from combined seismocardiography and gyrocardiography," *Sensors*, vol. 19, no. 16, p. 3472, 2019.

[3] J. Y. A. Foo and S. J. Wilson, "A computational system to optimise noise rejection in photoplethysmography signals during motion or poor perfusion states," *Medical and Biological Engineering and Computing*, vol. 44, no. 1, pp. 140–145, 2006.

[4] O. T. Inan, P.-F. Migeotte, K.-S. Park, M. Etemadi, K. Tavakolian, R. Casanella, J. Zanetti, J. Tank, I. Funtova, G. K. Prisk, *et al.*, "Ballistocardiography and seismocardiography: A review of recent advances," *IEEE J. biomedical and health informatics*, vol. 19, no. 4, pp. 1414–1427, 2014.

[5] J. Wahlström, I. Skog, P. Händel, F. Khosrow-Khavar, K. Tavakolian, P. K. Stein, and A. Nehorai, "A hidden markov model for seismocardiography," *IEEE TBME*, vol. 64, no. 10, pp. 2361–2372, 2017.

[6] M. J. Tadi, E. Lehtonen, T. Hurnanen, J. Koskinen, J. Eriksson, M. Pänkäälä, M. Teräs, and T. Koivisto, "A real-time approach for heart rate monitoring using a hilbert transform in seismocardiograms," *Physiological measurement*, vol. 37, no. 11, p. 1885, 2016.

[7] E. Chang, C.-K. Cheng, A. Gupta, P.-H. Hsu, P.-Y. Hsu, H.-L. Liu, A. Moffitt, A. Ren, I. Tsaur, and S. Wang, "Cuff-less blood pressure monitoring with a 3-axis accelerometer," in *2019 EMBC*. IEEE, 2019, pp. 6834–6837.

[8] K. Pandia, S. Ravindran, R. Cole, G. Kovacs, and L. Giovangrandi, "Motion artifact cancellation to obtain heart sounds from a single chest-worn accelerometer," in *2010 ICASSP*. IEEE, 2010, pp. 590–593.

[9] P.-Y. Hsu and C.-K. Cheng, "R-peak detection using a hybrid of gaussian and threshold sensitivity," in *2020 EMBC*. IEEE, 2020, pp. 4470–4474.